5-Aminoimidazole-4-Carboxamide-1-β-D-Ribofuranoside Causes Acute Hepatic Insulin Resistance In Vivo

R. Richard Pencek, Jane Shearer, Raul C. Camacho, Freyja D. James, D. Brooks Lacy, Patrick T. Fueger, E. Patrick Donahue, Wanda Snead, and David H. Wasserman

The infusion of 5-aminoimidazole-4-carboxamide-1-β-D-ribofuranoside (AICAR) causes a rise in tissue concentrations of the AMP analog 5-aminoimidazole-4-carboxamide-1-β-D-ribofuranotide (ZMP), which mimics an elevation of cellular AMP levels. The purpose of this work was to determine the effect of raising hepatic ZMP levels on hepatic insulin action in vivo. Dogs had sampling and infusion catheters as well as flow probes implanted 16 days before an experiment. After an 18-h fast, blood glucose was 82 ± 1 mg/dl and basal net hepatic glucose output 1.5 ± 0.2 $mg \cdot kg^{-1} \cdot min^{-1}$. Dogs received portal venous glucose (3.2 $mg \cdot kg^{-1} \cdot min^{-1}$), peripheral venous somatostatin, and basal portal venous glucagon infusions from −90 to 60 min. Physiological hyperinsulinemia was established with a portal insulin infusion (1.2 $mU \cdot kg^{-1} \cdot min^{-1}$). Peripheral venous glucose infusion was used to clamp arterial blood glucose at 150 mg/dl. Starting at $t = 0$ min, dogs received portal venous AICAR infusions of 0, 1, or 2 $mg \cdot kg^{-1} \cdot min^{-1}$. Net hepatic glucose uptake was 2.4 ± 0.5 $mg \cdot kg^{-1} \cdot min^{-1}$ (mean of all groups) before $t = 0$ min. In the absence of AICAR, net hepatic glucose uptake was 1.9 ± 0.4 mg $\cdot kg^{-1} \cdot min^{-1}$ at $t = 60$ min. The lower-dose AICAR infusion caused a complete suppression of net hepatic glucose uptake (−1.0 ± 1.7 $mg \cdot kg^{-1} \cdot min^{-1}$ at $t = 60$ min). The higher AICAR dose resulted in a profound shift in hepatic glucose balance from net uptake to a marked net output (−6.1 ± 1.9 $mg \cdot kg^{-1} \cdot min^{-1}$ at $t = 60$ min), even in the face of hyperglycemia and hyperinsulinemia. These data show that elevations in hepatic ZMP concentrations, induced by portal venous AICAR infusion, cause acute hepatic insulin resistance. These findings have important implications for the targeting of AMP kinase for the treatment of insulin resistance, using AMP analogs. *Diabetes* 54:355–360, 2005

From the Department of Molecular Physiology and Biophysics, Diabetes Research and Training Center, Vanderbilt University School of Medicine, Nashville, Tennessee.

Address correspondence and reprint requests to Richard Pencek, Department of Molecular Physiology and Biophysics, Vanderbilt University School of Medicine, Nashville, TN 37232-0615. E-mail: pencekr@dom.pitt.edu.

Received for publication 6 July 2004 and accepted in revised form 26 October 2004.

ACC, acetyl CoA carboxylase; AICAR, 5-aminoimidazole-4-carboxamide-1-β-D-ribofuranoside; NEFA, nonesterified fatty acid; ZMP, 5-aminoimidazole-4-carboxamide-1-β-D-ribofuranotide.

AICAR (5-aminoimidazole-4-carboxamide-1-β-D-ribofuranoside) is taken up by tissue adenosine transporters and phosphorylated to 5-aminoimidazole-4-carboxamide-1-β-D-ribofuranotide (ZMP)within the cell. This rise in intracellular ZMP mimics a rise in AMP (1). Treatment of healthy and diabetic rats with AICAR has been shown to increase fat and carbohydrate oxidation in skeletal muscle (2–4). The proposed target by which AICAR elicits its effects is AMP kinase. Considering the strong oxidative drive elicited by AICAR treatment, the targeting of AMP kinase has potential for the treatment of type 2 diabetes (5,6). In addition to activating AMP kinase, AICAR has also been shown to allosterically upregulate myocardial glycogen phosphorylase activity (7). This activation of glycogen phosphorylase may provide substrate for the oxidative effects of AICAR treatment. It has been postulated, based on work with Zucker rats, that AICAR treatment improves insulin action at the liver by enhancing insulin's ability to suppress hepatic glucose output (3,8). In contrast to these findings, it has been shown that hepatic AMP kinase activity is markedly increased during exercise, a state characterized by increased hepatic glucose production (9). Consistent with a role during exercise are rat studies showing that peripheral AICAR infusion causes an acute 50% reduction in liver glycogen (8). Recent work has also shown that treatment of hepatocytes with AICAR activates liver glycogen phosphorylase, even in the presence of elevations in glucose-6-phosphate (10). These data suggest that AICAR treatment opposes insulin action at the liver.

The role of AMP kinase stimulation in the liver remains unclear. Because AICAR treatment increases skeletal muscle glucose uptake, it could be a useful tool for lowering postprandial hyperglycemia in people with insulin resistance. However, its effects on insulin action in the liver remain to be carefully defined. Therefore, the purpose of this work was to determine the effects of AICAR on insulin-stimulated net hepatic glucose uptake in the presence of hyperglycemia and hyperinsulinemia characteristic of the postprandial state in a conscious, unstressed animal model.

RESEARCH DESIGN AND METHODS

A total of 18 mongrel dogs of either sex (mean weight 23 ± 1 kg) were housed in a facility that met the guidelines of the American Association for the Accreditation of Laboratory Animal Care. All surgical and experimental protocols were approved by the Vanderbilt University animal care and use committee. A laparotomy was performed on animals at least 16 days before an experiment, as previously described (11). Silastic infusion catheters were

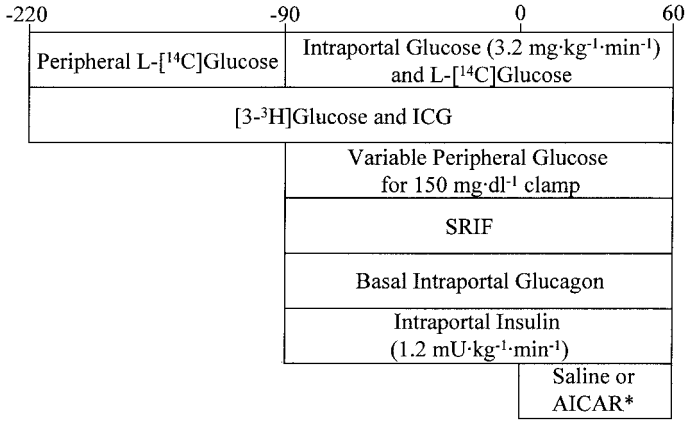

FIG. 1. Experimental protocol. Dogs were fasted 18 h before an experiment. After the establishment of a hyperinsulinemic-hyperglycemic clamp, dogs were infused with either saline ($n = 8$) or 1 mg · kg^{-1} · min^{-1} ($n = 5$) or 2 mg · kg^{-1} · min^{-1} of AICAR ($n = 5$). ICG, indocyanine green; SRIF, somatostatin. *1 or 2 mg · kg^{-1} · min^{-1}.

inserted into the inferior vena cava for the infusion of somatostatin (SRIF), glucose, indocyanine green, and radioactive isotopes of glucose ([3-^{3}H]glucose and L-[^{14}C]glucose). Infusion catheters were also inserted into the splenic and jejunal veins and fed forward into the portal vein for the infusion of insulin, glucagon, AICAR, glucose, and L-[^{14}C]glucose. Sampling catheters were inserted into the portal vein, hepatic vein, and femoral artery. Catheters were filled with saline containing heparin and knotted at the free end. Transonic flow probes (Transonic Systems, Ithaca, NY) were fitted to the hepatic artery and portal vein. Flow probe leads and the knotted catheter ends were placed in subcutaneous pockets. Animals that met the experiment inclusion criteria (good appetite [consumed entire daily ration], normal stool, white blood cell count <18,000, and hematocrit ≥0.35) were fasted 18 h before an experiment.

The experimental protocol is shown in Fig. 1. After the fasting period, the knotted catheter ends and flow probes were removed from the subcutaneous pockets with 1-cm incisions made under a local anesthetic (2% lidocaine). Dogs were then placed in a Pavlov harness, and the catheters were aspirated with saline. At $t = -220$ min, peripheral infusions of indocyanine green, [3-^{3}H]glucose, and L-[^{14}C]glucose were initiated. Indocyanine green was used for the determination of splanchnic blood flow in the event of flow probe failure. The infusion of [3-^{3}H]glucose continued for the duration of the experiment. The peripheral L-[^{14}C]glucose was terminated at −90 min. From $t = -120$ to −90 min, baseline blood samples were taken. At $t = -90$ min, a peripheral infusion of SRIF was initiated to suppress pancreatic insulin and glucagon secretion. Basal circulating levels of glucagon were maintained with a portal glucagon infusion (0.5 ng · kg^{-1} · min^{-1}). Physiological hyperinsulinemia was established with 1.2 mU · kg^{-1} · min^{-1} intraportal insulin infusion. Also at $t = -90$ min, glucose was infused (3.2 mg · kg^{-1} · min^{-1}) into the portal vein. L-[^{14}C]glucose was added to the portal glucose infusion to establish the same tracer infusion rate as that used for the peripheral infusion before $t = -90$ min. A variable peripheral glucose infusion was used to clamp arterial blood glucose concentrations at 150 mg/dl. After the initiation of these infusions, 80 min was allotted for the establishment of steady-state conditions. At $t = -10$ and 0 min, blood samples were taken for assessment of substrate concentration and hepatic substrate balance. After the $t = 0$ min sample, dogs received either 1 mg · kg^{-1} · min^{-1} (AICAR1 group, $n = 5$) or 2 mg · kg^{-1} · min^{-1} (AICAR2 group, $n = 5$) portal AICAR infusion from $t = 0$ to 60 min. Control animals (saline group, $n = 8$) were treated identically to the AICAR1 and AICAR2 groups, except that AICAR was not infused. These animals served as time controls. Six of the eight control dogs were previously described (11) and did not have the −10 and 0 min samples. Blood samples were taken every 10 min after the onset of saline or AICAR. At 60 min, dogs were killed, and liver biopsies were frozen in liquid nitrogen.

Plasma, blood, and tissue analyses. Plasma glucose levels were determined during experiments via the glucose oxidase method, using a Glucose Analyzer II (Beckman Instruments, Fullerton, CA). Plasma and tissue samples that were not immediately analyzed were stored at −70°C. Whole-blood samples were deproteinized with barium hydroxide and zinc sulfate and then centrifuged (3,000*g* for 30 min), and the supernatant was dried. Samples were reconstituted in 1 ml of water and 10 ml Ultima Gold scintillant (Packard, Meriden, CT), and radioactivity was determined using a Packard Tri-Carb 2900TR liquid scintillation counter. Plasma insulin and glucagon were measured using previously described radioimmunoassay techniques (12,13). Liver glycogen concentration and radioactivity (14) and liver glycogen phosphorylase and synthase activities (15) were determined as described previously. For the determination of hepatic glucose-6-phosphate and fructose-6-phosphate levels, liver samples where homogenized in 8% perchloric acid and centrifuged (3,000*g* for 10 min). Blood glucose and hepatic concentrations of glycogen (after digestion of precipitated glycogen with amyloglucosidase), glucose-6-phosphate, and fructose-6-phosphate were measured using enzymatic methods on a Technicon autoanalyzer (16). Hepatic adenine nucleotide and ZMP concentrations were determined from liver samples homogenized in 0.4 mol/l perchloric acid/0.5 mmol/l EGTA and neutralized with 0.5 mol/l potassium carbonate, pH 6.8. High-performance liquid chromatography analysis and UV detection was performed to assess nucleotide levels, as previously described (17,18).

Western analysis. Liver samples were homogenized in a solution containing: 10% glycerol, 20 mmol/l Na-pyrophosphate, 150 mmol/l NaCl, 50 mmol/l HEPES (pH 7.5), 1% NP-40, 20 mmol/l β-glycerophosphate, 10 mmol/l NaF, 2 mmol/l EDTA (pH 8.0), 2 mmol/l phenylmethylsulfonyl fluoride, 1 mmol/l $CaCl_2$, 1 mmol/l $MgCl_2$, 10 μg/ml aprotinin, 10 μg/ml leupeptin, 2 mmol/l Na_2VO_3, and 3 mmol/l benzamide. Homogenized samples were assayed for protein concentration using a Pierce BCA protein assay kit (Rockford, Il). Next, 30 μg of protein was run on an SDS-PAGE gel and transferred to a polyvinylidene difluoride membrane. Membranes were treated with rabbit α-phospho-AMP kinase-α (Thr172) or α-phospho-acetyl CoA carboxylase (Cell Signaling, Beverly, MA) and then incubated with α-rabbit–horseradish peroxidase (Promega, Madison, WI). Chemiluminescence was detected with a WesternBreeze kit from Invitrogen (Carlsbad, CA). Densitometry was performed using LabImage software (National Institutes of Health).

Calculations. Net hepatic glucose balance was calculated using the following equation: ([A] − [H]) × HAF + ([P] − [H]) × PVF, where [A], [H], and [P] represent blood glucose concentrations of the artery, hepatic vein, and portal vein, respectively. HAF and PVF represent the hepatic artery and portal vein blood flows, respectively. Positive values obtained from this equation represent net hepatic glucose uptake, whereas negative values represent output. Net hepatic glycogen deposition was calculated as the amount of [3-^{3}H]glucose radioactivity incorporated into glycogen per mass tissue divided by the inflowing specific activity. Inflowing specific activity was calculated as: ([P*] × PVF + [A*] × HAF)/([P] × PVF + [A] × HAF). In this equation, [P*] and [A*] represent portal and arterial [3-^{3}H]glucose radioactivity (dpm/ml), respectively.

Mixing of glucose in the portal vein was assessed using L-[^{14}C]glucose (11). The appearance of L-[^{14}C]glucose was calculated by multiplying the difference in radioactivity in the artery and portal vein by the portal vein flow. Studies were considered mixed if at least half of the time points had an L-[^{14}C]glucose appearance rate within ±30% of the actual infusion rate.

Statistical analysis. All dogs received identical treatment before the infusion of AICAR. Data before the experimental period that were pooled after statistical analyses showed no differences between groups. Comparisons within a group and between groups were made using ANOVA and repeated-measures ANOVA. Differences were considered significant when $P < 0.05$.

RESULTS

Baseline values in the 18-h–fasted dog. After an 18-h fast, arterial blood glucose was 82 ± 1 mg/dl and net hepatic glucose output 1.5 ± 0.2 mg · kg^{-1} · min^{-1} ($n = 18$). Arterial plasma insulin and glucagon concentrations were typical of the short-term fasted state (Table 1). Arterial plasma cortisol, epinephrine, and norepinephrine concentrations suggest the animals were unstressed (Table 2). Arterial lactate, alanine, glycerol, and nonesterified

TABLE 1
Arterial plasma insulin and glucagon concentrations prior to and during the saline and AICAR infusion experimental period

	Pre-experimental	Experimental
Insulin (μU/ml)		
Saline	23 ± 3	22 ± 3
AICAR1	18 ± 4	22 ± 3
AICAR2	22 ± 2	28 ± 2
Glucagon (ng/l)		
Saline	28 ± 7	29 ± 6
AICAR1	52 ± 10	45 ± 8
AICAR2	26 ± 6	27 ± 4

Data are means ± SE.

TABLE 2
Arterial plasma cortisol, epinephrine, and norepinephrine concentrations during the hyperisulinemic-hyperglycemic clamp in the presence of saline or AICAR infusions

	Saline	AICAR1	AICAR2
Cortisol (μg/dl)	2.6 ± 0.4	3.0 ± 0.3	1.9 ± 0.5
Epinephrine (pg/ml)	139 ± 27	101 ± 14	88 ± 15
Norepinephrine (pg/ml)	149 ± 23	167 ± 41	202 ± 12

Data are means ± SE.

fatty acid (NEFA) concentrations were 577 ± 59, 350 ± 28, 69 ± 10, and 773 ± 106 μmol/l, respectively.

Hyperinsulinemic-hyperglycemic clamp period. Insulin levels rose approximately threefold compared with baseline levels during the hyperinsulinemic-hyperglycemic clamp period (Table 1). The infusion of AICAR did not alter insulin levels. During the hyperinsulinemic-hyperglycemic clamp, similar arterial blood glucose levels of 150 mg/dl were established in all groups (Fig. 2). Arterial plasma glucagon was similar to baseline during the clamp with or without AICAR. Arterial cortisol, epinephrine, and norepinephrine concentrations were also similar during the hyperinsulinemic-hyperglycemic clamp in the presence or absence of AICAR (Table 2).

The liver switched from net output of glucose during the baseline period to net uptake during the hyperinsulinemic-hyperglycemic clamp (Fig. 3). Before AICAR, net hepatic glucose uptake was 2.4 ± 0.5 mg · kg^{-1} · min^{-1} at t = 0 min. In the saline group, net hepatic glucose uptake was sustained over the course of the clamp (1.9 ± 0.4 mg · kg^{-1} · min^{-1} at t = 60 min). Net hepatic glucose uptake was completely suppressed in the AICAR1 group (−1.0 ± 1.7 mg · kg^{-1} · min^{-1} at t = 60 min). Net hepatic glucose uptake was not only completely suppressed in the AICAR2 group, but it showed marked output (−6.1 ± 1.9 mg · kg^{-1} · min^{-1} at t = 60 min), despite the presence of both elevated insulin and glucose.

Before the AICAR infusion period, the glucose infusion rate required to maintain the hyperglycemic clamp was ~9 mg · kg^{-1} · min^{-1} (sum of all groups). The change in the glucose infusion rate required to maintain the clamp after the onset of saline or AICAR infusion is shown in Fig. 4. In saline-infused dogs, the glucose infusion rate gradually rose during the experimental period. After the onset of AICAR infusion, the glucose infusion rate fell significantly by 1.8 ± 0.6 mg · kg^{-1} · min^{-1} in the AICAR1 group and 3.3 ± 1.4 mg · kg^{-1} · min^{-1} in the AICAR2 group by t = 60 min.

During the hyperinsulinemic-hyperglycemic clamp period, lactate levels were 729 ± 119 μmol/l in the saline group and were not altered by AICAR infusion (707 ± 86

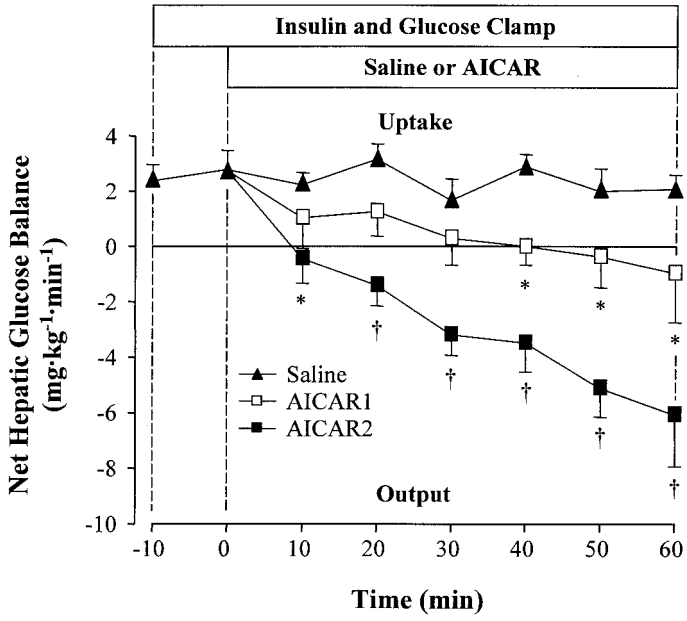

FIG. 3. Net hepatic glucose balance during the insulin hyperinsulinemic-hyperglycemic clamp before and during the saline (saline group) or 1 mg · kg^{-1} · min^{-1} (AICAR1 group) or 2 mg · kg^{-1} · min^{-1} (AICAR2 group) AICAR infusions. Positive values reflect net uptake, and negative values reflect net output. Data are means ± SE. *P < 0.05 vs. saline; †P < 0.05 vs. the saline and AICAR1 groups.

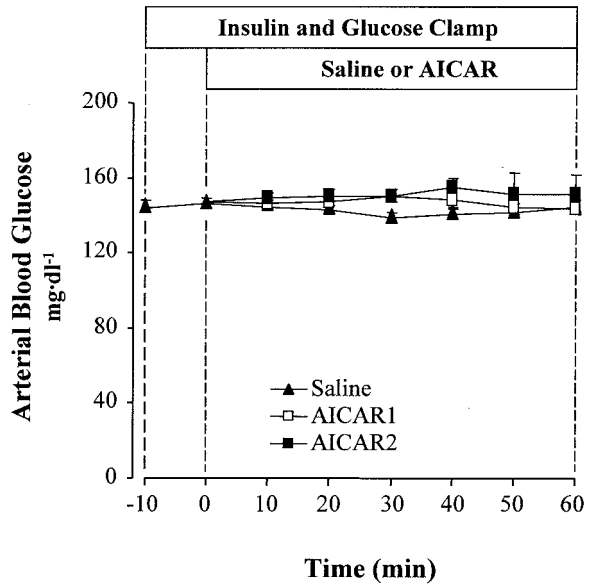

FIG. 2. Arterial blood glucose during the insulin clamp period before and during saline or 1 mg · kg^{-1} · min^{-1} (AICAR1 group) or 2 mg · kg^{-1} · min^{-1} (AICAR2 group) AICAR infusions. Data are means ± SE.

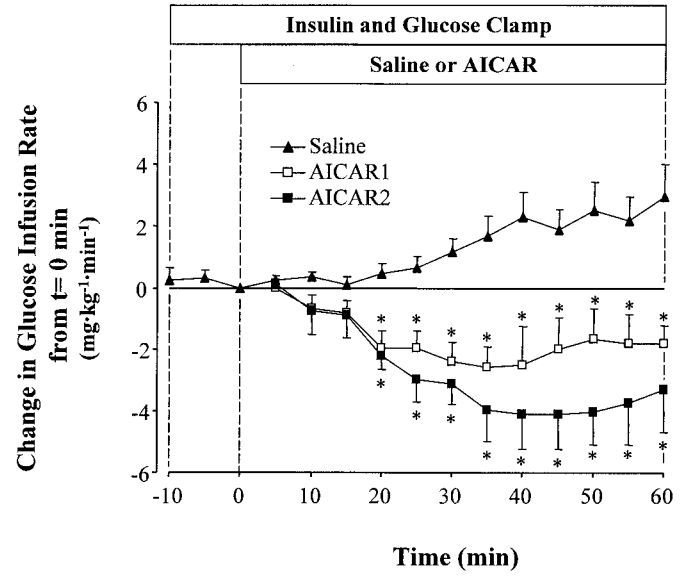

FIG. 4. The change in glucose infusion rate during the saline (saline group) or 1 mg · kg^{-1} · min^{-1} (AICAR1 group) or 2 mg · kg^{-1} · min^{-1} (AICAR2 group) AICAR infusions. Data are the means ± SE. *P < 0.05 vs. saline.

TABLE 3
Liver net glycogen deposited, glucose-6-phosphate, fructose-6-phosphate, glycogen synthase (activity ratio), and glycogen phosphorylase (activity ratio)

	Saline	AICAR1	AICAR2
Net glycogen deposition (mg/g tissue)	4.2 ± 0.7	2.3 ± 0.5*	1.0 ± 0.1*†
Glycogen synthase (activity ratio)	0.20 ± 0.03	0.24 ± 0.02	0.20 ± 0.01
Glycogen phosphorylase (activity ratio)	0.60 ± 0.04	0.70 ± 0.06	0.71 ± 0.05
Glucose-6-phosphate (mg/100 g tissue)	5.2 ± 0.8	12.1 ± 1.8*	12.0 ± 4.1*
Fructose-6-phosphate (mg/100 g tissue)	1.9 ± 0.2	3.6 ± 0.7*	3.6 ± 1.2*

Data are means ± SE. *$P \leq 0.05$ vs. saline; †$P \leq 0.05$ vs. AICAR1.

and 689 ± 74 μmol/l in the AICAR1 and AICAR2 groups, respectively). Likewise, alanine levels were similar in the saline group (285 ± 20 μmol/l) and in AICAR-infused dogs (385 ± 76 and 253 ± 36 μmol/l in the AICAR1 and AICAR2 groups, respectively). In the presence of the hyperinsulinemic-hyperglycemic clamp, arterial glycerol levels fell to similar levels in both the saline group (27 ± 7 μmol/l) and the AICAR-infused animals (20 ± 6 and 10 ± 7 μmol/l in the AICAR1 and AICAR2 groups, respectively). In a manner similar to glycerol, arterial NEFAs fell to similar levels in the saline group (82 ± 16 μmol/l) and the AICAR-infused dogs (139 ± 44 and 163 ± 65 μmol/l in the AICAR1 and AICAR2 groups, respectively). During the hyperinsulinemic-hyperglycemic clamp, net hepatic balances (μmol · kg^{-1} · min^{-1}; positive values reflecting uptake) of lactate (−5.5 ± 1.5, −12.5 ± 6, and −8.3 ± 0.9), alanine (1.9 ± 0.41, 2.7 ± 1.4, and 2.5 ± 0.6), glycerol (0.73 ± 0.27, 0.23 ± 0.04, and 0.29 ± 0.14), and NEFA (0.15 ± 0.22, 0.41 ± 0.22, and 0.69 ± 0.5) were similar in the saline, AICAR1, and AICAR2 groups, respectively.

Liver glycogen synthesis, phosphorylase/synthase activities, glucose-6-phosphate, and fructose-6-phosphate concentrations. Net glycogen deposition was reduced by ~45% in the AICAR1 compared with the saline group (Table 3). In the AICAR2 group, net hepatic glycogen deposition was reduced by ~75% compared with the saline group and was significantly lower than that seen in the AICAR1 group. Insignificant trends reflecting increases in glycogen phosphorylase activity were present with AICAR infusions. AICAR had no effect on hepatic glycogen synthase activity. Liver glucose-6-phosphate and fructose-6-phosphate levels were elevated in the AICAR1 and AICAR2 groups.

Liver purine nucleotide levels. ZMP levels were undetectable in the absence of AICAR (Table 4). AICAR infusion resulted in dose-dependent increases in hepatic ZMP. Hepatic AMP levels were significantly reduced in the AICAR1 group. The AICAR2 group showed an insignificant reduction in hepatic AMP levels ($P = 0.145$). Hepatic ADP and ATP levels were also reduced by low- and high-dose AICAR infusions.

TABLE 4
Liver nucleotide concentrations (μmol/g liver)

	Saline	AICAR1	AICAR2
ZMP	ND	2.36 ± 0.57*	6.57 ± 1.87*†
AMP	0.65 ± 0.09	0.37 ± 0.06*	0.45 ± 0.05
ADP	0.87 ± 0.10	0.43 ± 0.05*	0.20 ± 0.01*
ATP	1.59 ± 0.12	0.65 ± 0.12*	0.65 ± 0.07*

ND, not detectable. *$P \leq 0.05$ vs. saline; †$P \leq 0.05$ vs. AICAR1.

Western analysis. Densitometry and representative Western blots of phosphorylated acetyl CoA carboxylase (ACC) are shown in Fig. 5. AICAR did not cause a significant increase in phospho-AMP kinase at either dose (data not shown). However, the downstream target of AMP kinase, ACC, showed a significant increase in phosphorylation in both the AICAR1 and AICAR2 groups.

DISCUSSION

This work demonstrates that portal venous AICAR infusion potently suppresses net hepatic glucose uptake in the presence of elevated insulin and glucose levels. Indeed, with the high-dose AICAR infusion (2 mg · kg^{-1} · min^{-1}), net hepatic glucose uptake was not only suppressed, but the liver switched to marked net output. In fact, the rate of output (~6 mg · kg^{-1} · min^{-1}) was as high as rates evident during stress or exercise (19). The results of the current study are consistent with AICAR impacting the regulation of liver glycogen. Low-dose AICAR infusion caused a ~45% reduction in net liver glycogen deposition, whereas the higher-dose AICAR infusion resulted in a ~75% reduction. Considering that these reductions occurred with a rise in liver glucose-6-phosphate and fructose-6-phosphate and an increase in liver glucose production, it is likely that glycogen synthesis was inhibited by increasing glycogenolysis. The glycogenolytic response to AICAR infusion could have been mediated by the allosteric effects of ZMP on glycogen phosphorylase, activation of AMP kinase, or a combination of both (10). These findings are consistent with the observation that hepatic glycogen stores were reduced by 50% 2 h after a bolus of AICAR (8), reflecting a

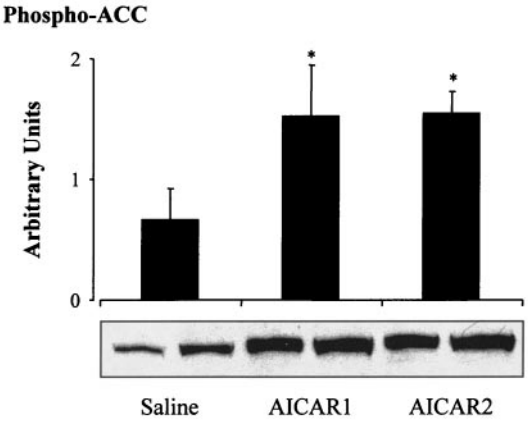

FIG. 5. Representative Western blot and densitometry analysis for liver phospho-ACC. The blots show two representative analyses from each group. Densitometry analysis is the means ± SE for all dogs in the saline, AICAR1, and AICAR2 groups. Data are the means ± SE. *$P \leq 0.05$ vs. the saline group.

large net glycogenolytic response. The findings reported here are also consistent with the observation that the glucose infusion rate during an insulin clamp is decreased after administration of a primed AICAR infusion (5 mg/kg bolus, 3.75 mg · kg^{-1} · min^{-1} infusion) in the rat (20).

The effect of AICAR infusion on gluconeogenesis is also of important consideration. AICAR infusion inhibits hepatic fatty acid synthesis and stimulates fatty acid oxidation, which would seemingly promote gluconeogenesis (21). However, work in dominant-negative AMP kinase–expressing rats has shown that the activation of AMP kinase by adiponectin can lower plasma glucose (22). The work goes on to describe experiments in hepatocytes that implicate downregulation of PEPCK and glucose-6-phosphatase expression as a likely mechanism for the improvement in plasma glucose. Additionally, work in glycogen-reduced liver cells has shown that AICAR treatment reduces hepatic glucose production (23). This finding indicates that AICAR treatment has a suppressive effect on gluconeogenesis; however, it is unclear whether such an effect on hepatic glucose production occurs in the presence of substantial hepatic glycogen stores. In the current study, there were no differences in arterial concentrations or net hepatic balances of NEFA, lactate, alanine, or glycerol between saline- and AICAR-infused dogs, which suggests that increased gluconeogenesis did not contribute significantly to the switch from net hepatic glucose uptake to net hepatic glucose output seen with AICAR infusion.

Although there was no apparent increase in phospho-AMP kinase, the downstream target of AMP kinase, ACC, showed a significant increase in phosphorylation. Given that AMP kinase activity is regulated by both allosteric interactions as well as phosphorylation, phosphorylation of ACC is a more sensitive marker of AMP kinase activity (24–26). This notion is supported by work in myocardial tissue showing that AICAR treatment resulted in a clear increase in the phosphorylation of ACC, with little or no detectable change in phosphorylation of AMP kinase (7).

Muscle AMP kinase activation facilitates the uptake and oxidation of substrates as well as mobilizes muscle glycogen stores, and it may play a role in the postexercise sensitization of muscle to insulin stimulation (4,7,27,28). These actions of AMP kinase are consistent with a role in coordinating the metabolic response in working muscle. Interestingly, work has shown that during exercise, AMP kinase activity increases in the liver as well (9). During exercise, liver glucose output increases to help meet the increasing energy demands of working muscle (19). This increase in hepatic glucose output results from increased glycogenolysis mediated by a fall in portal vein insulin and a rise in portal vein glucagon (29,30). One may postulate that increases in AMP and/or AMP kinase signaling mediate this effect. Considering that glycogenolysis in muscle and liver are both increased during exercise and AMP kinase activity is increased in both tissues, it is reasonable to postulate that AMP kinase activation may play a role in the glycogenolytic response to exercise seen in both tissues.

Elevations in ZMP cause phosphorylation and activation of AMP kinase in a manner identical to that of AMP, i.e., by both allosteric mechanisms and inducing the phosphorylation of AMP kinase (31). Additionally, ZMP mimics the allosteric effects of AMP in the regulation of phosphorylase activity at least in myocardial tissue (7). Work performed in lean and obese Zucker rats using a peripheral AICAR infusion indicated that an infusion of 10 mg · kg^{-1} · min^{-1} (with a primer bolus of 100 mg/kg) suppresses endogenous glucose production (3). In the Zucker diabetic fatty rat, a peripheral venous bolus of AICAR resulted in an improved ability of insulin to suppress hepatic glucose output 24 h later (8). In the present study, AICAR was infused directly into the portal vein at a rate that was 10–20% of that used in rodent models. Portal venous AICAR infusion allows for more direct targeting of the drug to the liver while minimizing peripheral effects of the drug.

The allosteric actions of ZMP binding activate glycogen phosphorylase in a manner identical to that of AMP (7). Elevations in AMP within the physiological range have been shown to activate liver glycogen phosphorylase (32) and override the inhibitory effect of glucose on glycogen phosphorylase (33). Additionally, recent work in cultured hepatocytes has shown that incubation with 0.2–0.3 mmol/l AICAR causes marked activation of glycogen phosphorylase (10). In the current study, the infusion of AICAR produced hepatic ZMP levels 4- and 10-fold higher than the levels of hepatic AMP seen during the saline infusion. This elevation in ZMP was enough to counterbalance the inhibitory effect of hyperglycemia on glycogen phosphorylase. In this experiment there was an 18% increase in phosphorylase activity in AICAR2. However, the change was insignificant ($P = 0.07$). It should be noted that this assay takes into account the activity of the enzyme and not the subcellular localization. It is possible that the 18% increase in phosphorylase activity combined with potential changes in the distribution of the phosphorylase enzyme is sufficient to stimulate glycogenolysis. Support for the notion that glycogen phosphorylase plays a critical role in the regulation of glycogen synthesis comes from metabolic control analysis, where it was shown that phosphorylase activity has a strong control coefficient with regard to glycogen synthesis (34).

These findings show that portal venous AICAR infusion for 60 min, at 1 or 2 mg · kg^{-1} · min^{-1}, causes marked resistance to insulin-stimulated net hepatic glucose uptake. Insulin-stimulated net hepatic glucose uptake was completely alleviated, and at the higher dose, AICAR actually increased liver glucose output to 6 mg · kg^{-1} · min^{-1}. This insulin resistance is characterized by a reduction in the glucose infusion rate to maintain the hyperglycemic clamp. The results of this work are consistent with the work of Camacho et al. (34a), which showed that portal AICAR infusion (1 mg · kg^{-1} · min^{-1}) stimulated hepatic glucose production in the presence of basal intraportal glucagon, hyperinsulinemia, and either euglycemia or hypoglycemia. Previous work has shown that AICAR causes marked improvements in muscle glucose uptake and oxidation (3,8,35–37). Additionally, AICAR increases the production of the antidiabetic adipokine adiponectin (38). Although these improvements have been well documented, it is important to note that these improvements occurred in animals receiving acute or chronic AICAR treatment via either injections or peripheral infusions. It is possible that human work will show similar improvements using injections or peripheral infusions. However, the route of drug delivery will be a very important consider-

ation if AICAR, or drugs with similar actions, are developed for human use. Oral administration, the preferred method for chronic use, designed to produce a given arterial concentration would result in much higher hepatic concentrations, which likely would result in hepatic effects closer to the marked increases in hepatic glucose production that were seen in the present study, provided that the liver contains appreciable glycogen stores.

In conclusion, the results of this work show that AICAR infusion causes a marked suppression of net hepatic glucose uptake in the presence of elevated insulin and glucose, and it can even cause the liver to become a net producer of glucose. These findings have important implications. First, they add new emphasis to a possible role of purine nucleotides in the regulation of hepatic glycogen metabolism and hepatic glucose output. Second, the results of these studies are important to consider when evaluating the potential use of AMP analogs in the treatment of diabetes.

REFERENCES

1. Corton JM, Gillespie JG, Hawley SA, Hardie DG: 5-Aminoimidazole-4-carboxamide ribonucleoside: a specific method for activating AMP-activated protein kinase in intact cells? *Eur J Biochem* 229:558–565, 1995
2. Bergeron R, Russell RR 3rd, Young LH, Ren JM, Marcucci M, Lee A, Shulman GI: Effect of AMPK activation on muscle glucose metabolism in conscious rats. *Am J Physiol* 276:E938–E944, 1999
3. Bergeron R, Previs SF, Cline GW, Perret P, Russell RR 3rd, Young LH, Shulman GI: Effect of 5-aminoimidazole-4-carboxamide-1-β-D-ribofuranoside infusion on in vivo glucose and lipid metabolism in lean and obese Zucker rats. *Diabetes* 50:1076–1082, 2001
4. Musi N, Goodyear LJ: AMP-activated protein kinase and muscle glucose uptake. *Acta Physiol Scand* 178:337–345, 2003
5. Winder WW: AMP-activated protein kinase: possible target for treatment of type 2 diabetes. *Diabetes Technol Ther* 2:441–448, 2000
6. Musi N, Goodyear LJ: Targeting the AMP-activated protein kinase for the treatment of type 2 diabetes. *Curr Drug Targets Immune Endocr Metabol Disord* 2:119–127, 2002
7. Longnus SL, Wambolt RB, Parsons HL, Brownsey RW, Allard MF: 5-Aminoimidazole-4-carboxamide 1-beta-D-ribofuranoside (AICAR) stimulates myocardial glycogenolysis by allosteric mechanisms. *Am J Physiol Regul Integr Comp Physiol* 284:R936–R944, 2003
8. Iglesias MA, Ye JM, Frangioudakis G, Saha AK, Tomas E, Ruderman NB, Cooney GJ, Kraegen EW: AICAR administration causes an apparent enhancement of muscle and liver insulin action in insulin-resistant high-fat–fed rats. *Diabetes* 51:2886–2894, 2002 (Erratum in *Diabetes* 52:223–224, 2003)
9. Carlson CL, Winder WW: Liver AMP-activated protein kinase and acetyl-CoA carboxylase during and after exercise. *J Appl Physiol* 86:669–674, 1999
10. Aiston S, Green A, Mukhtar M, Agius L: Glucose 6-phosphate causes translocation of phosphorylase in hepatocytes and inactivates the enzyme synergistically with glucose. *Biochem J* 377:195–204, 2004
11. Pencek RR, James F, Lacy DB, Jabbour K, Williams PE, Fueger PT, Wasserman DH: Interaction of insulin and prior exercise in control of hepatic metabolism of a glucose load. *Diabetes* 52:1897–1903, 2003
12. Morgan CR, Lazarow AL: Immunoassay of insulin: two antibody system: plasma insulin of normal, subdiabetic, and diabetic rats. *Am J Med Sci* 257:415–419, 1963
13. Hamilton KS, Gibbons FK, Bracy DP, Lacy DB, Cherrington AD, Wasserman DH: Effect of prior exercise on the partitioning of an intestinal glucose load between splanchnic bed and skeletal muscle. *J Clin Invest* 98:125–135, 1996
14. Chan T, Exton J: A rapid method for the determination of glycogen content and radioactivity in small quantities of tissue or isolated hepatocytes. *Anal Biochem* 71:96–105, 1976
15. Golden S, Wals PA, Katz J: An improved procedure for the assay of glycogen synthase and phosphorylase in rat liver homogenates. *Anal Biochem* 77:436–445, 1977
16. Lloyd B, Burrin J, Smythe P, Alberti KG: Enzymatic fluorometric continuous-flow assays for blood glucose, lactate, pyruvate, alanine, glycerol, and 3-hydroxybutyrate. *Clin Chem* 24:1724–1729, 1978
17. Wynants J, Van Belle H: Single-run high-performance liquid chromatography of nucleotides, nucleosides, and major purine bases and its application to different tissue extracts. *Anal Biochem* 144:258–266, 1985
18. Ally A, Park G: Rapid determination of creatine, phosphocreatine, purine bases and nucleotides (ATP, ADP, AMP, GTP, GDP) in heart biopsies by gradient ion-pair reversed-phase liquid chromatography. *J Chromatogr* 575:19–27, 1992
19. Wasserman DH, Cherrington AD: Hepatic fuel metabolism during exercise: role and regulation. *Am J Physiol* 260:E811–E824, 1991
20. Bradley E, Zhang L, Newman J, Richards S, Clark M, Rattigan S: Acute, divergent effects of AICAR on insulin action in vivo (Abstract). *Diabetes* 52 (Suppl. 1):A344, 2003
21. Merrill GF, Kurth EJ, Hardie DG, Winder WW: AICA riboside increases AMP-activated protein kinase, fatty acid oxidation, and glucose uptake in rat muscle. *Am J Physiol* 273:E1107–E1112, 1997
22. Yamauchi T, Kamon J, Minokoshi Y, Ito Y, Waki H, Uchida S, Yamashita S, Noda M, Kita S, Ueki K, Eto K, Akanuma Y, Froguel P, Foufelle F, Ferre P, Carling D, Kimura S, Nagai R, Kahn BB, Kadowaki T: Adiponectin stimulates glucose utilization and fatty-acid oxidation by activating AMP-activated protein kinase. *Nat Med* 8:1288–1295, 2002
23. Zhou G, Myers R, Li Y, Chen Y, Shen X, Fenyk-Melody J, Wu M, Ventre J, Doebber T, Fujii N, Musi N, Hirshman MF, Goodyear LJ, Moller DE: Role of AMP-activated protein kinase in mechanism of metformin action. *J Clin Invest* 108:1167–1174, 2001
24. Winder WW: Energy-sensing and signaling by AMP-activated protein kinase in skeletal muscle. *J Appl Physiol* 91:1017–1028, 2001
25. Hutber CA, Hardie DG, Winder WW: Electrical stimulation inactivates muscle acetyl-CoA carboxylase and increases AMP-activated protein kinase. *Am J Physiol* 272:E262–E266, 1997
26. Al-Khalili L, Krook A, Zierath JR, Cartee GD: Prior serum- and AICAR-induced AMPK activation in primary human myocytes does not lead to subsequent increase in insulin-stimulated glucose uptake. *Am J Physiol Endocrinol Metab* 287:E553–E557, 2004
27. Wojtaszewski JF, Jorgensen SB, Hellsten Y, Hardie DG, Richter EA: Glycogen-dependent effects of 5-aminoimidazole-4-carboxamide (AICA)-riboside on AMP-activated protein kinase and glycogen synthase activities in rat skeletal muscle. *Diabetes* 51:284–292, 2002
28. Musi N, Yu H, Goodyear LJ: AMP-activated protein kinase regulation and action in skeletal muscle during exercise. *Biochem Soc Trans* 31:191–195, 2003
29. Wasserman DH, Lacy DB, Goldstein RE, Williams PE, Cherrington AD: Exercise-induced fall in insulin and hepatic carbohydrate metabolism during exercise. *Am J Physiol* 256:E500–E508, 1989
30. Wasserman DH, Spalding JS, Lacy DB, Colburn CA, Goldstein RE, Cherrington AD: Glucagon is a primary controller of the increments in hepatic glycogenolysis and gluconeogenesis during exercise. *Am J Physiol* 257:E108–E117, 1989
31. Aschenbach WG, Hirshman MF, Fujii N, Sakamoto K, Howlett KF, Goodyear LJ: Effect of AICAR treatment on glycogen metabolism in skeletal muscle. *Diabetes* 51:567–573, 2002
32. Ercan-Fang N, Gannon MC, Rath VL, Treadway JL, Taylor MR, Nuttall FQ: Integrated effects of multiple modulators on human liver glycogen phosphorylase a. *Am J Physiol Endocrinol Metab* 283:E29–E37, 2002
33. Ercan N, Gannon MC, Nuttall FQ: Allosteric regulation of liver phosphorylase a: revisited under approximated physiological conditions. *Arch Biochem Biophys* 328:255–264, 1996
34. Aiston S, Hampson L, Gomez-Foix AM, Guinovart JJ, Agius L: Hepatic glycogen synthesis is highly sensitive to phosphorylase activity: evidence from metabolic control analysis. *J Biol Chem* 276:23858–23866, 2001

34a. Camacho RC, Pencek RR, Lacy DB, James FD, Donahue EP, Wasserman DH: Portal venous 5-aminoimidazole-4-carboxamide-1-β-D-ribofuranoside infusion overcomes hyperinsulinemic suppression of endogenous glucose output. *Diabetes* 54:373–382, 2005

35. Buhl ES, Jessen N, Schmitz O, Pedersen SB, Pedersen O, Holman GD, Lund S: Chronic treatment with 5-aminoimidazole-4-carboxamide-1-β-D-ribofuranoside increases insulin-stimulated glucose uptake and GLUT4 translocation in rat skeletal muscles in a fiber type–specific manner. *Diabetes* 50:12–17, 2001
36. Buhl ES, Jessen N, Pold R, Ledet T, Flyvbjerg A, Pedersen SB, Pedersen O, Schmitz O, Lund S: Long-term AICAR administration reduces metabolic disturbances and lowers blood pressure in rats displaying features of the insulin resistance syndrome. *Diabetes* 51:2199–2206, 2002
37. Halseth AE, Ensor NJ, White TA, Ross SA, Gulve EA: Acute and chronic treatment of ob/ob and db/db mice with AICAR decreases blood glucose concentrations. *Biochem Biophys Res Commun* 294:798–805, 2002
38. Lihn AS, Jessen N, Pedersen SB, Lund S, Richelsen B: AICAR stimulates adiponectin and inhibits cytokines in adipose tissue. *Biochem Biophys Res Commun* 316:853–858, 2004